Design for a GeV per meter, laser-driven electron accelerator

Y.C. Huang, and R.L. Byer

Stanford Univeristy, Edward Ginzton Laboratory
Stanford, CA 94305-4085

ABSTRACT

We propose a dielectric-based, multistaged, laser-driven electron linear accelerator microstructure operating in a vacuum that is capable of accelerating electrons to 1 TeV in one kilometer. Our study shows that a GeV/m gradient is achievable using two 100 fsec focused crossed-laser-beams, repeated every 300 μm, operated at a peak power of 0.2 GW and an energy density of less than $2J/\mathrm{cm}^2$ on the accelerator structure.

Keywords: accelerator, laser, integrated optics, high power laser, laser-driven accelerator, ultra-fast laser, crossed-laser-beam accelerator, short pulse laser

In a conventional S-band RF accelerator, field emission on the copper wall occurs when the peak acceleration gradient reaches ~100 MeV/m[1]. The average acceleration gradient for an RF accelerator is thus limited to about 50 MeV/m. To reach the TeV energy region desired for the next linear collider using presently existing RF schemes requires tens of kilometers of accelerator structure.

The laser accelerator gradient, like the RF accelerator gradient, is limited by damage. Figure 1a shows that dielectric materials, which are commonly used for optical components, have a damage fluence an order of magnitude higher than copper[2,3]. Derived from Fig. 1a, Fig. 1b illustrates that the damage threshold field and thus the maximum acceleration gradient on the dielectric surface can be as high as 10 GV/m for 100 fsec pulse lasers. A laser accelerator structure using dielectric boundaries is therefore an appealing scheme for achieving GeV/m gradients and for building future TeV electron accelerators at existing laboratory sites.

In this paper, we propose a crossed-laser-beam accelerator structure and evaluate its feasibility with current laser technology. Similar schemes were discussed in several papers[4,5,6], but no accelerator structure was presented. In calculating the GeV/m gradient, we take into account several practical considerations such as laser damage, the drift space occupied by optical components, and the geometrical limitation for coupling laser beams into the structure.

The Lawson-Woodward (LW) theorem[7,8] rules out the possibility of a net energy gain for a relativistic electron interacting linearly with electromagnetic waves in an unbounded vacuum. In the following, the proposed accelerator structure consists of repetitive dielectric boundaries over a distance no greater than a π phase slip between the laser field and the electron in a vacuum.

Figure 2a shows the proposed crossed-laser-beam accelerator geometry, wherein an electron traverses the focal zone at an angle θ with respect to the two laser beams. The insert in Fig. 2a defines the coordinates used in this paper. The two laser beams are derived from a single laser source, carry equal power, and are phased such that on the z axis the transverse fields (in x and y) cancel and the longitudinal fields (in z) add.

Figure 2b shows a single stage of the proposed dielectric accelerator optical configuration. Two laser beams are back-reflected from the $\pm x$ directions into the microstage using two prisms. The total internal reflection (TIR) inside the prisms permits the use of anti-reflection (AR) coatings for beam coupling.

0-8194-2075-1/96/$6.00

Two high-reflectivity coated flat mirrors provide a secondary reflection and direct the two laser beams into the center of the microstage. The back-reflection scheme allows the coupling points (labeled A and A') on the prisms to be away from the z axis so that the laser beam clipping at the prism edges can be minimized. Beam clipping at the prism determines the geometrical beam coupling condition given by

$$3l \times \theta > w, \tag{1}$$

where l is half of the interaction length measured from the focal point, and w is the Gaussian beam electric field beam radius at A and A'. For a small angle θ, a minimum prism width (in z) of $2w$ is required for coupling $> 90\%$ of the laser power into the structure. Thus the minimum drift space per microstage, where no laser fields exist, is approximately $2w$. The proposed structure can be constant in y which allows cylindrical focusing if necessary.

A linearly polarized fundamental Gaussian beam can be described by a vector potential polarized in x with Gaussian profiles in the x' and y' [9]. The two electric field components that are important to the on-axis electrons are $E_{x'}$ and $E_{z'}$. With the appropriate coordinate transformation, the electrical field seen by an on-axis electron, summed from $E_{x'}$ and $E_{z'}$ of the two crossed laser beams, is

$$E_z = -4\sqrt{\frac{\eta P}{\pi}} \frac{\sin\theta}{w_0(1+z^2/z_r^2 \times \cos^2\theta)} \exp\left[-\frac{(z/w_0 \times \sin\theta)^2}{1+z^2/z_r^2 \times \cos^2\theta}\right] \cos(\phi_p + \phi_g + \phi_r), \tag{2}$$

where η is the wave impedance in vacuum, P is the laser power, w_0 is the laser waist size, $z_r = \pi w_0^2/\lambda$ is the optical Rayleigh length, and ϕ_p, ϕ_g, ϕ_r are the plane wave phase, Guoy phase term, and radial phase, respectively. For a relativistic electron with an energy γ and a small crossing angle $\theta << 1$, the three phase terms are

$$\phi_p = \omega t - kz\cos\theta \approx \frac{kz}{2}(\theta^2 - \frac{1}{\gamma^2}), \tag{3}$$

$$\phi_g = 2 \times \tan^{-1}(z/z_r), \tag{4}$$

$$\text{and } \phi_r = -\frac{(z/z_r) \times (z\theta/w_0)^2}{1+z^2/z_r^2}. \tag{5}$$

The small angle assumption, $\theta << 1$, is necessary for achieving phase coherence over a distance much longer than an optical wavelength. However, for highly relativistic electrons with $1/\gamma^2 << \theta^2$, the plane wave phase shift can be reduced to $\phi_p \approx kz\theta^2/2$. A typical Gaussian field carries a Guoy phase[10], $\tan^{-1}(z/z_r)$, which gives a π phase shift from $z = -\infty$ to $z = \infty$. However, in Eq. (4) an additional Guoy phase is contributed from summing $E_{x'}$ and $E_{z'}$. The sum of the plane wave phase and radial phase terms is $\phi_p + \phi_r = \frac{z \times z_r(\theta/w_0)^2}{1+(z/z_r)^2}$, which has the same sign as the Guoy phase term. Since the Guoy phase term, $2 \times \tan^{-1}(z/z_r)$, produces a π phase shift from $-z_r$ to $+z_r$, net acceleration is possible only if the laser field is terminated for $z < |z_r|$.

For an on-axis electron, the energy gain from $-l$ to $+l$ is the integration of the longitudinal electric field over the distance:

$$\Delta W = \int_{-l}^{l} E_z \cdot dz. \tag{6}$$

By careful evaluation, it can be shown that the maximum energy gain for an on-axis electron is $\Delta W_{\max}(\mathrm{MeV}) = 30\sqrt{P(\mathrm{TW})}$, with a crossing angle $\theta = 1.37 \times w_0/z_r$ and an interaction length $2l = 0.92 z_r$, corresponding to a π phase slip in the accelerator stage. However the laser power is limited by the laser-induced damage on optical components and by the geometric coupling condition in Eq. (1).

The optical damage fluence and thus the acceleration gradient depends on the laser pulse length such that a short laser pulse is desirable for obtaining a high acceleration gradient[2]. For example, with a 100 fsec pulse length, the damage threshold intensity is about $I_{\max} = 20\mathrm{TW/cm}^2$, at a damage threshold fluence[3] of $\sim 2\,J/\mathrm{cm}^2$. The maximum laser power $P_{\max}$ at the damage threshold intensity $I_{\max}$ is given by $P_{\max} = I_{\max} w^2 \pi/2$.

In practice, the critical parameter is not the maximum energy gain per microstage but the average acceleration gradient. We define the average acceleration gradient as the energy gain per stage, ΔW, divided by the repeat length of an accelerator stage, $L_\mu = 2l + 2w$. Substituting $P_{\max}$ into (6) and dividing (6) by L_μ, one has the average acceleration gradient under the laser damage constraint given by

$$G = \left.\frac{\Delta W}{L_\mu}\right|_{P = I_{\max} w^2 \pi/2}. \tag{7}$$

In Eq. (7), the variables are the interaction length 2l, the laser waist radius w_0, the crossing angle θ, and the optical wavelength λ. We assume the wavelength λ = 1 μm for the rest of our calculations.

Figure 3 shows the average acceleration gradient versus the interaction length per stage *2l*, for w_0 = 20 μm and θ = 100 mrad, 70 mrad, and 40 mrad. When the interaction length equals zero, the average gradient is reduced to zero instead of converging to the electric field strength at the focal point, because a finite drift distance of 2w per stage is taken into account in Eq. (7). The solid curves satisfy the geometrical constraint in Eq.(1). For θ = 100 mrad and 70 mrad, average gradients approaching 1 GeV/m are predicted. In the same plot a smaller angle, θ = 40 mrad, gives a maximum average gradient of ~ 0.65 GeV/m. Note that for θ = 40 mrad the acceleration gradient is less sensitive to the interaction length, which can be as long as ~ 300 μm. A larger structure size eases the fabrication process, reduces the radiation loss, allows a larger electron channel, and opens the fabrication tolerance. We thus evaluated the G = 0.7 GeV/m contours on the θ and w_0 space (indicated by solid lines in Fig. 4) for different interaction lengths 2l subject to the geometric constraint of Eq. (1) (indicated by dashed lines in Fig. 4) and the damage fluence of $2\,J/cm^2$ for a 100 fsec laser drive. The (w_0, θ) pairs complying with the geometric constraint are those indicated by the bold dark lines in Fig. 4. It is seen that for an interaction length longer than 340 μm no operation point on the contours is available due to the violation of the geometric constraint. We found in our computer simulation that electron energy spread and emittance growth are predominantly caused by a large crossing angle θ. Therefore point A in Fig. 3, where $L_\mu \approx 2l + 2w_0$ = 334 μm, w_0 = 17 μm, and θ = 42 mrad, can be the optimum operation point for 0.7 GeV/m accelerator design.

Figure 5 shows the schematic of a multistage accelerator that can be integrated on a silicon wafer by using the low-cost, high-precision lithographic technology. The phase of the laser fields is controlled by

electro-optic phase controllers and the group velocity delay is controlled with slabs of dielectric. If necessary, microactuators or micromotors can be integrated into the same wafer in a batch process. The dimensions are consistent with the optimum parameters found on the 0.7 GeV/m average gradient contours. Optical components occupy approximately 10% of the length in the electron acceleration direction. In Fig. 5, we assume that a plane wave is incident on each focusing lens and thus a nominal 7mm × 34μm elliptical beam profile from a single laser source may drive 20 microstages simultaneously. A dielectric channel of a few microns can be opened for transmitting the electrons. For GeV electron beams, it has been demonstrated that the transverse beam size can be as small as 75 nanometers[11].

Precise phase locking of individual lasers is necessary for multi-macrostage acceleration. Locking the phase between two CW solid-state lasers has been demonstrated in the past[12]. The principle of a mode-locked laser is essentially the same as that of a CW laser except that there is a fixed phase relationship among the longitudinal modes in a mode-locked laser. We believe locking the phase between two mode-locked lasers is achievable without undue difficulty.

When the electrons propagate through the dielectric channel of each accelerator stage, the electrons lose their kinetic energy to transition radiation. Moreover, the impact field, the static field carried by each electron, could damage the dielectric structure at high γ. Both radiation loss and impact field induced damage impose limitation on the number of electrons in each optical cycle. One scheme to circumvent the limitation is spreading electrons evenly in the y direction. Indeed, accelerating a line charge by using cylindrical laser focusing has additional advantages such as reducing the phase slip due to diffraction, reducing the beamstrahlung at the final electron focusing, and assisting heat dissipation. In our calculation, an electron density of $1.1 \times 10^7/\text{mm}$ can be accelerated up to 1 TeV energy at 10% radiation loss.

Future work includes the study of beam loading, wake field issues, and multi-stage particle dynamics.

REFERENCES

[1] E. Tanabe, "Microwave Field Emission", Applied Surface Science, v76-77, 16 (1994).
[2] D. Zheng, R.L. Byer, "Proposed Waveguide Structure for Laser Driven Electron Accelerator," in *Proc. 6th Workshop on Advanced Accelerator Concepts*, Fontana, Wisconsin, June 12-18, 1994 .
[3] B.C. Stuart, M.D. Feit, A.M. Rubenchik, B.W. Shore, and M.D. Perry, *Phy. Rev. Let.* v 74 n12, 2248 (1995).
[4] T. Hauser, W. Scheid, and H. Hora, "Acceleration of Electrons by Intense Laser Pulses in Vacuum", Phys. Lett. A 186, 189 (1994).
[5] C.M. Haaland, "Laser Electron Acceleration in Vacuum", Opt. Comm. 114, 280 (1995).
[6] P. Sprangle, E. Esarey, J. Krall, and A. Ting, "Vacuum Laser Acceleration," to be published in Opt. Comm.
[7] J.D. Lawson, "Laser and Accelerators", IEEE Trans. Nucl. Sci. Vol. NS-26, No.3, 4217 (1979).
[8] P.M. Woodward, *J IEE* **93**, 1554 (1947).
[9] L.W. Davis, "Theory of Electromagnetic Beams", Physical Rev. A Vol. 19, No. 3, 1177 (1979).
[10] A.E. Siegman, *Lasers*, (Mill Valley, California 1986), p.683.
[11] B. Schwarzschil, "New Stanford Facility Squeezes High-energy Electron Beams," Physics Today, July 1994, p. 22.
[12] T. Day, E.K. Gustafson, and R.L. Byer, "Sub-hertz relative Frequency Stabilization of Two-diode laser-pumped Nd:YAG lasers Locked to a Fabry-Perot Interferometer", IEEE J. Quan. Elec. vol. QE-18, no. 4, 1106 (1992).

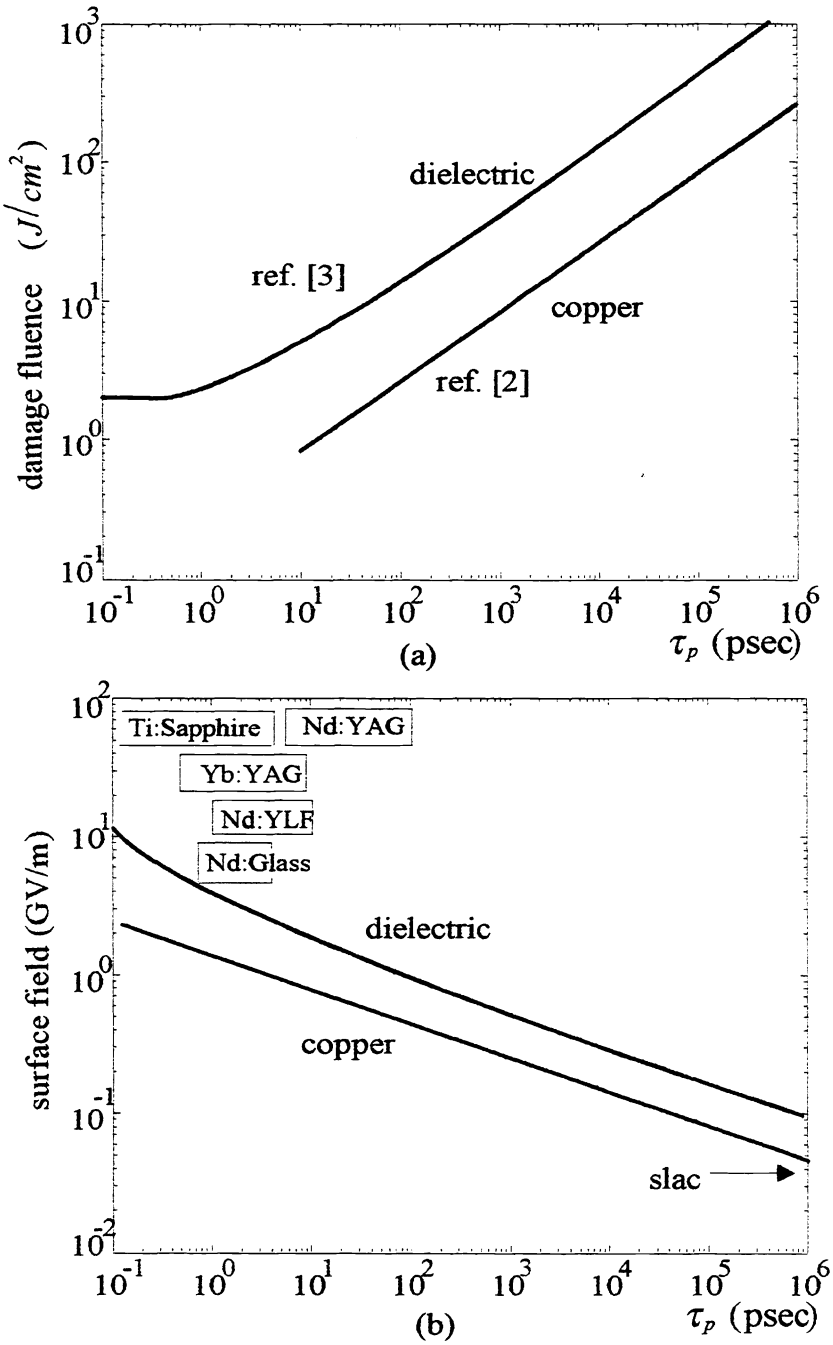

Figure 1. (a) Damage threshold fluence for a dielectric and copper versus laser pulse length. The dielectric can sustain a fluence that is one order of magnitude higher than copper. (b) Surface field strength (the maximum acceleration gradient) at damage threshold. Laser sources that operate at the corresponding pulse lengths are indicated on the graph.

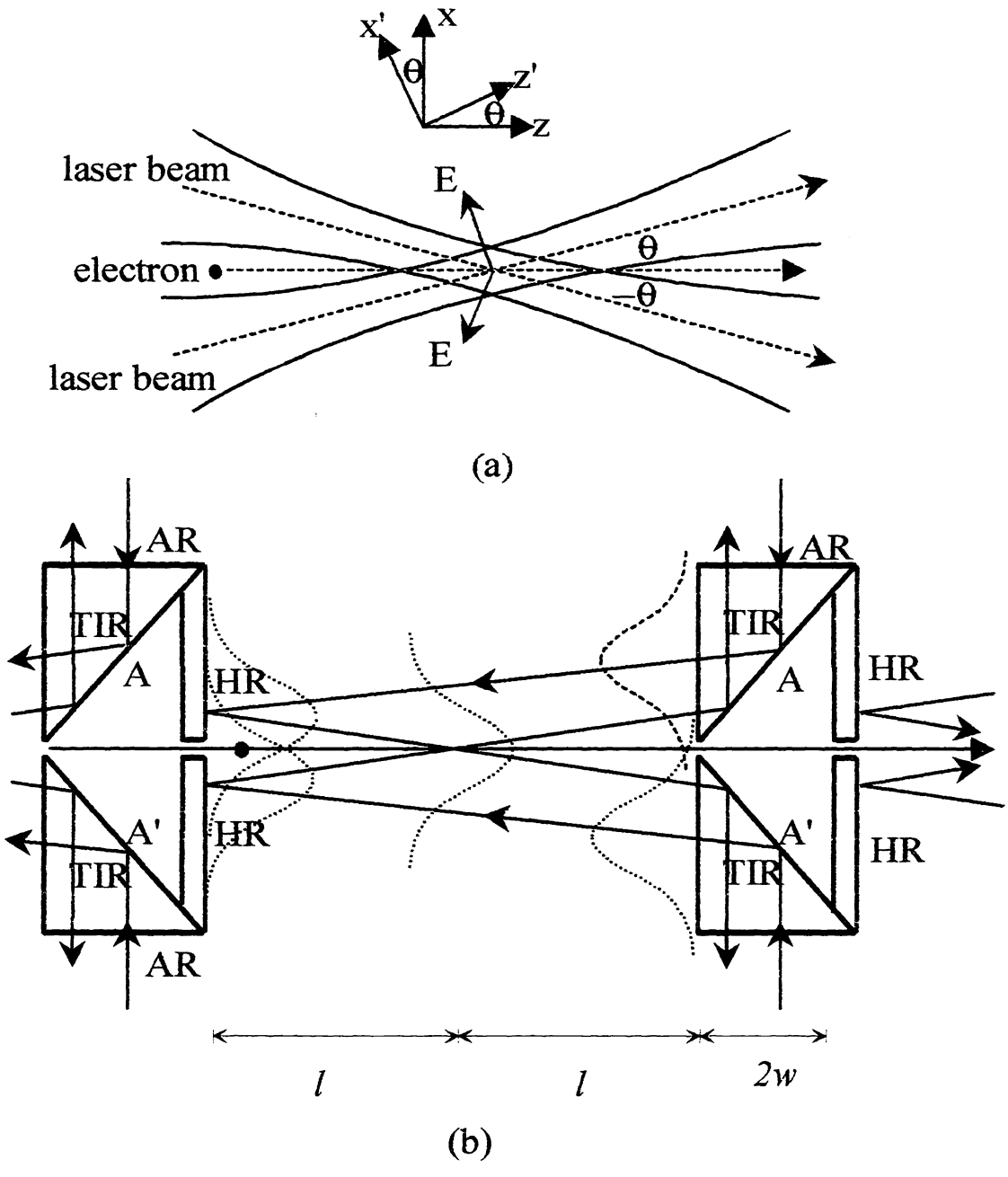

Figure 2 (a) The schematic for a crossed-laser-beam accelerator. The electron traverses the focal zone at an angle θ with respect to each of the two beams. The two laser beams are phased such that the longitudinal fields add and the transverse fields cancel. (b) The back-reflection scheme for a single microstage. This scheme avoids clipping the laser beam at the coupling prisms when θ is small. The drift space occupied by optical components for each microstage is approximately two laser spot sizes, $2w$.

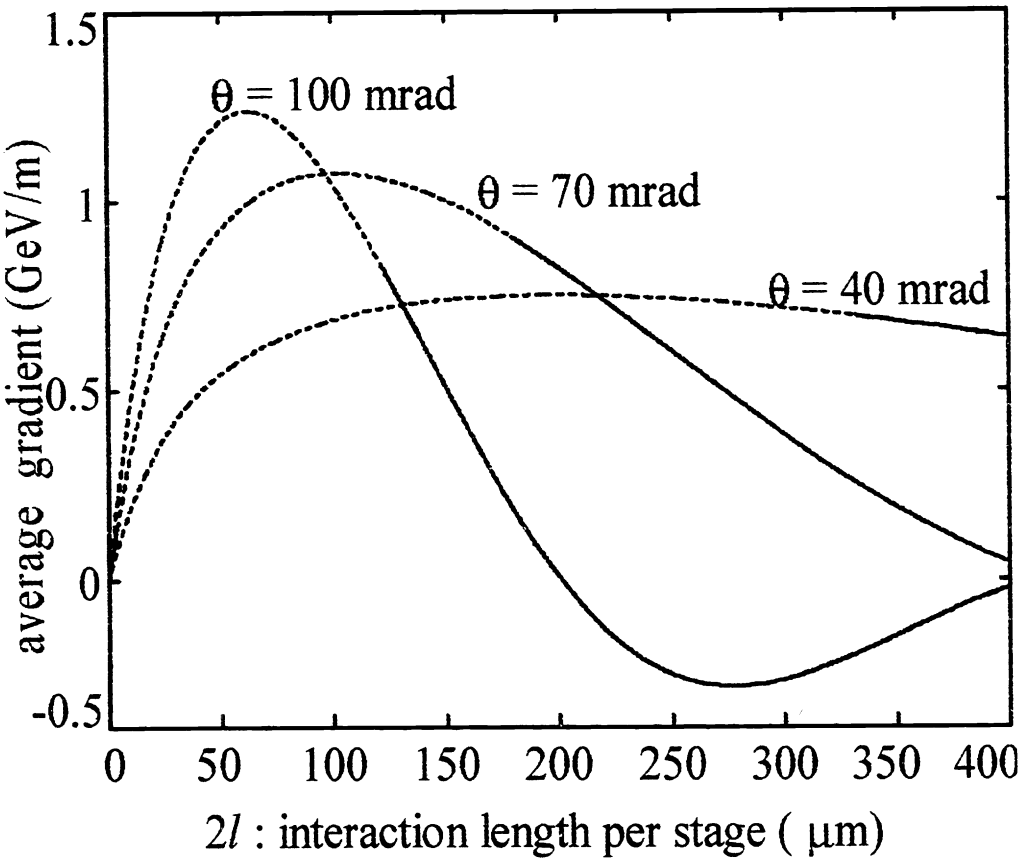

Figure 3. Average acceleration gradient versus acceleration length for various crossing angles. Gradients approaching 1 GeV/m are predicted. The solid lines satisfy the geometric constraint of Eq. (1).

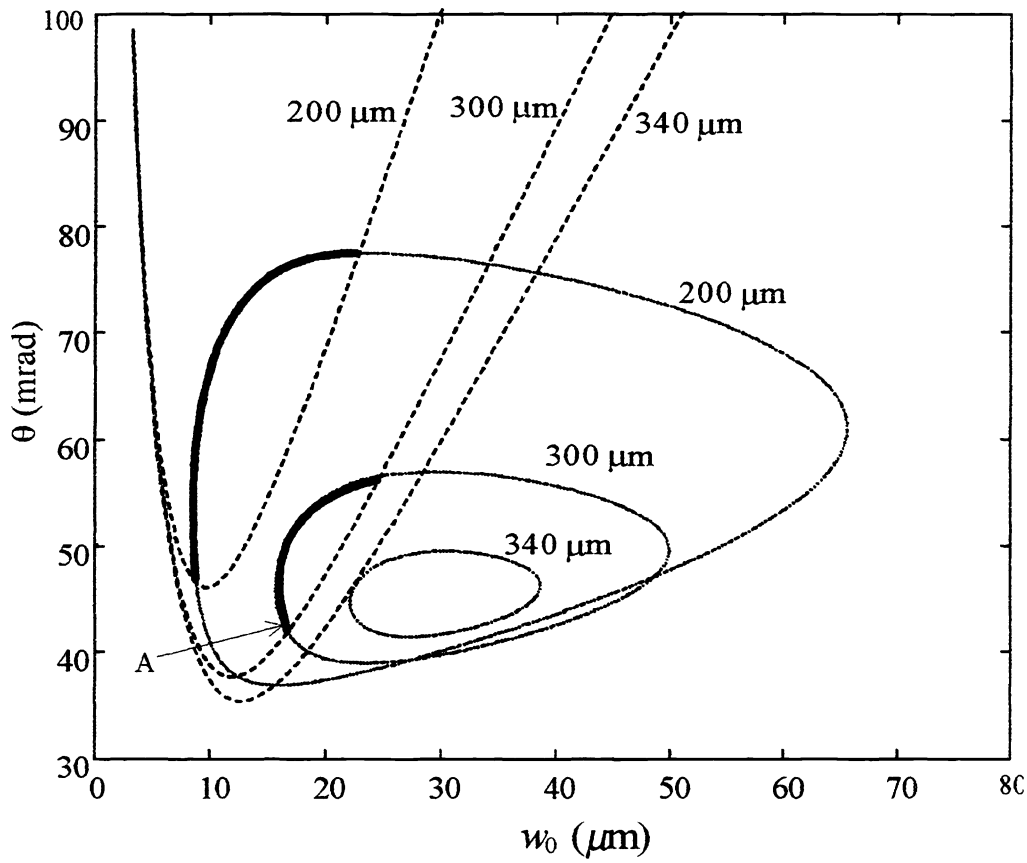

Figure 4. 0.7 GeV/m contours on the θ versus w_0 plane for various interaction lengths, 2l. The parabolic curves are calculated from Eq. (1) for the same 2l. The allowed (θ, w_0) pairs are those on the contours and above the corresponding parabolic curves. Point A gives the smallest electron energy spread and emittance in computer simulation.

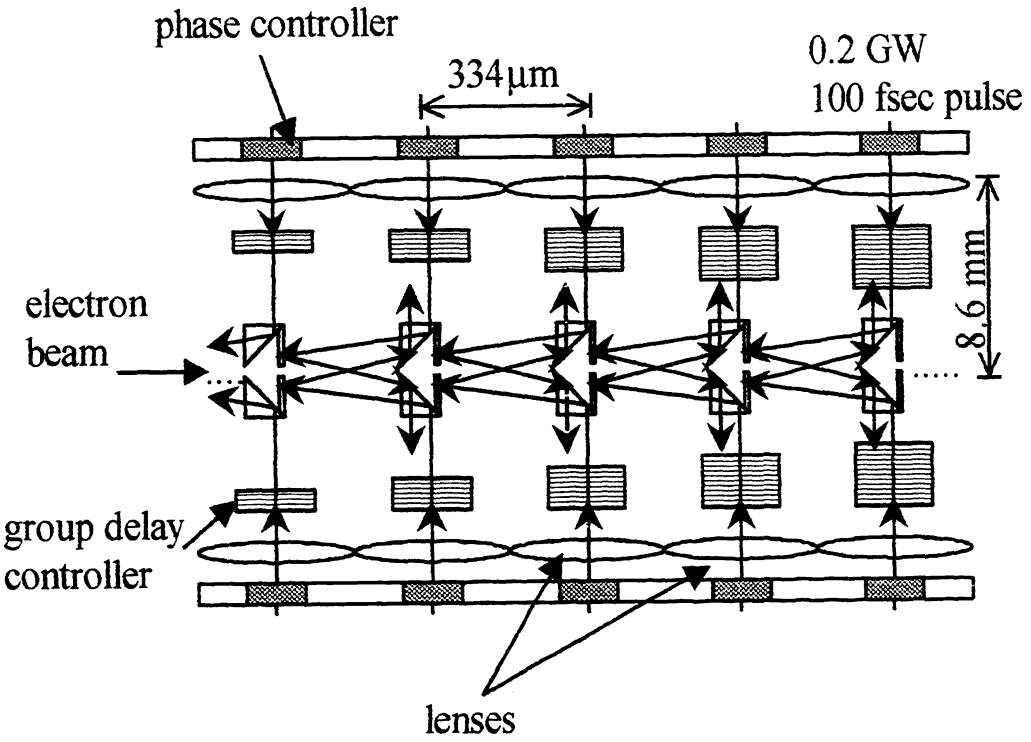

Figure 5. A multistage accelerator that can be integrated on a silicon wafer using lithographic technology. The phase of laser fields is controlled by electro-optic phase controllers and the group velocity delay is controlled with slabs of dielectric.